International Journal of Remote Sensing
Vol. 29, No. 4, 20 February 2008, 1007–1027

Taylor & Francis
Taylor & Francis Group

Improved topographic correction of forest image data using a 3-D canopy reflectance model in multiple forward mode

S. A. SOENEN*†, D. R. PEDDLE†, C. A. COBURN†, R. J. HALL†‡ and F. G. HALL§

†Department of Geography, University of Lethbridge, 4401 University Drive West, Lethbridge, AB, Canada T1K 3M4

‡Canadian Forest Service, Northern Forest Centre, 5320 – 122 Street, Edmonton, AB, Canada T6H 3S5

§NASA Goddard Space Flight Centre, Code 614.4, 8800 Greenbelt Rd., Greenbelt MD 20771, USA

(*Received 23 August 2006; in revised form 13 February 2007*)

In most forestry remote sensing applications in steep terrain, simple photometric and empirical (PE) topographic corrections are confounded as a result of stand structure and species assemblages that vary with terrain and the anisotropic reflective properties of vegetated surfaces. To address these problems, we present MFM-TOPO as a new physically-based modelling (PBM) approach for normalising topographically induced signal variance as a function of forest stand structure and sub-pixel scale components. MFM-TOPO uses the Li-Strahler geometric optical mutual shadowing (GOMS) canopy reflectance model in Multiple Forward Mode (MFM) to account for slope and aspect influences directly. MFM-TOPO has an explicit physical-basis and uses sun-canopy-sensor (SCS) geometry that is more appropriate than strictly terrain-based corrections in forested areas since it preserves the geotropic nature of trees (vertical growth with respect to the geoid) regardless of terrain, view and illumination angles. MFM-TOPO is compared against our recently developed SCS+C correction and a comprehensive set of other existing PE and SCS methods (cosine, *C* correction, Minnaert, statistical-empirical, SCS, and *b* correction) for removing topographically induced variance and for improving SPOT image classification accuracy in a Rocky Mountain forest in Kananaskis, Alberta Canada. MFM-TOPO removed the most terrain-based variance and provided the greatest improvement in classification accuracy within a species and stand density based class structure. For example, pine class accuracy was increased by 62% over shaded slopes, and spruce class accuracy was increased by 13% over more moderate slopes. In addition to classification, MFM-TOPO is suitable for retrieving biophysical parameters in mountainous terrain.

1. Introduction

Remote sensing image analysis can be compromised by the radiometric influence of topography on recorded sensor signals (Smith *et al.* 1980, Justice *et al.* 1981, Teillet *et al.* 1982, Meyer *et al.* 1993, Peddle *et al.* 2003a, Soenen *et al.* 2005). In areas of varying topography, calibrated reflectance values for satellite and aerial imagery are

*Corresponding author. Email: scott.soenen@uleth.ca

International Journal of Remote Sensing
ISSN 0143-1161 print/ISSN 1366-5901 online
http://www.tandf.co.uk/journals
DOI: 10.1080/01431160701311291

not solely representative of the intrinsic surface cover physical properties, but are also influenced by the slope and aspect of the surface on which they are found (Teillet *et al.* 1982). This is especially the case in forested terrain where topography affects both the sun-canopy-sensor (SCS) geometry and shading within the canopy (Gu and Gillespie 1998, Soenen *et al.* 2005). Thus, the variation in reflectance as a result of changes in important physical characteristics such as species and density may be less than the reflectance variation from differences in topographic orientation. This can lead to image classification error (Itten and Meyer 1992, Meyer *et al.* 1993, Gu *et al.* 1999) as well as error in forest physical-structural estimates (Gemmell 1995, 1998, Johnson *et al.* 2000).

A number of correction methods have been developed to reduce the topographic effect in optical remotely sensed imagery in forested terrain, as reviewed in Peddle *et al.* (2003a) and Soenen *et al.* (2005) and summarized here. These can be categorized into two main types of corrections: photometric/empirical (PE) and sun-canopy sensor (SCS) corrections, with the latter providing the foundation for a third and different approach presented here, that of physically-based models (PBM). Early PE approaches were based on a Lambertian assumption and applied photometric correction factors or empirical models to raw image data prior to any reflectance calibration. This provided a simple and generalized correction in forested terrain where the correction to the sensor data was based solely on the inferred relationship between radiance (L) and incidence angle (i, defined as the angle between the illumination source and a line perpendicular to the terrain surface). Problems with the sun-terrain-sensor (STS) geometry of PE approaches led to the development of SCS corrections set in a more appropriate geometrical framework. The major PE and SCS methods are reviewed briefly in the next section to set the context for our PBM approach. Regardless of approach, however, the goal of any topographic correction in forested terrain is to simplify the connection between physical-structural conditions within forest stands with respect to the signal recorded at the sensor, by diminishing or removing the relationship between L and i. Thus, a topographically corrected image should have no observed relationship between terrain orientation and recorded signal for forest stands with identical or similar structure. After a correction, any signal variance should be explained by species and stand structure or typical remote sensing error sources, but not by terrain orientation.

1.1 *Photometric and empirical (PE) topographic correction methods*

The first and most general PE topographic correction is the cosine correction, which for a constant solar zenith angle corrects radiance based on Lambert's cosine law (Smith *et al.* 1980). The cosine model applies a correction factor based on the angle of incidence to the radiance data. Due to the simplicity of this model, the effect of diffuse illumination is not accounted for, resulting in overestimation of the output radiance data (Teillet *et al.* 1982), and in some cases, large errors. Corrections such as the C correction and Minnaert correction (Teillet *et al.* 1982) have been more appropriate for rugged terrain since they included moderators to the simple cosine correction that improved the effectiveness of the model over steep, shaded slopes (Meyer *et al.* 1993, Peddle *et al.* 2003a). The Minnaert correction included the empirically derived k constant (Minnaert 1941), which gives an indication of the level of anisotropic scattering for a non-Lambertian surface, while the C correction included another additive empirical constant to simulate the effect of diffuse

irradiance. Other correction methods have been developed which rely on empirical equations based on the relationship between image data and the angle of incidence. These corrections are either based on a linear relationship with radiance, as is the case with the statistical empirical correction (Teillet *et al.* 1982, Meyer *et al.* 1993), or a linear relationship with the natural logarithm of radiance values, as with the *b*-correction (Vincini and Frazzi 2003).

1.2 *Sun-canopy-sensor (SCS) corrections*

The Lambertian framework of the PE correction methods has been shown, both theoretically and empirically, to be inappropriate in forested terrain (Gu and Gillespie 1998, Peddle *et al.* 2003a Soenen *et al.* 2005). PE methods are based on sun-terrain-sensor geometry, however, in forest stands this does not properly characterize the sun-surface-sensor geometry since trees on slopes are not normal to the surface. Accordingly, improved correction models were developed based on SCS geometry that preserves the geotropic nature of trees (vertical growth with respect to the geoid) regardless of terrain, view and illumination angles. Thus, in the SCS method, irradiance and exitance angle are not affected by the underlying topographic slope on individual sunlit tree crowns (Gu and Gillespie 1998). The underlying terrain does, however, affect the relative positioning of trees within the canopy and the resulting sunlit and shadowed crown area, the fundamental drivers of pixel level reflectance in forested terrain. The SCS correction model is therefore more appropriate in forested terrain since it normalizes the area of sunlit canopy rather than the underlying terrain (Gu and Gillespie 1998).

However, the SCS model, like the simple cosine correction, is subject to overcorrection effects in steep, shaded terrain. Thus, Soenen *et al.* (2005) introduced and validated a new SCS + C correction, in which the addition of the *C* parameter (Teillet *et al.* 1982) to the SCS framework served to moderate the overcorrection found at larger incidence angles. The C parameter is additive, similar to the effect of diffuse irradiance. In Soenen *et al.* (2005), a synthesized dataset served as the basis for validation of this SCS + C correction, for which SCS + C was more appropriate for forested terrain than SCS and all four other photometric and empirical corrections considered (cosine, *C*, statistical empirical, Minnaert).

1.3 *Physically-based model (PBM) correction*

Although SCS corrections are based on the normalization of sunlit canopy area, they still do not fully explain the relationship between terrain, crown structure, shadowing and mutual shadowing within a forest stand and tree canopies. Forest stands of different species and structure vary with respect to the amount of cast shadow introduced by neighbouring tree crowns over varying terrain. Thus, an explicit, structure-specific topographic correction is desirable (Peddle *et al.* 2003a).

Therefore, to more appropriately describe and correct for the effect of topography in forested stands, it is necessary to apply a more sophisticated correction model possessing an explicit and more detailed characterization of canopy structure and terrain geometry. This type of approach should describe the primary factors contributing to stand-level radiance (Li and Strahler 1992) such as the proportions of sub-pixel scale shadow (canopy and understory), sunlit canopy, and sunlit understory, as a function of terrain orientation. These three sub-pixel components

have a more complex relationship with terrain orientation than that represented by simple photometric models (Cavayas and Teillet 1985, Schaff *et al.* 1992).

Fortunately, models of an appropriate level of complexity for this task exist for forested terrain (Chen *et al.* 2000). These models require additional inputs of physical canopy structure so that instead of the simple photometric model for a constant illumination angle, where normalized radiance (L_n) is a function of terrain geometry (g):

$$L_n = Lf(g) \tag{1}$$

the correction becomes a function of both geometry and canopy structure (cs):

$$L_n = Lf(g, cs) \tag{2}$$

To apply this complex correction model it is necessary to use general cs information for a given pixel. While empirical structural parameters are often unavailable, this structural information can be estimated instead using an indirect inversion process to facilitate this type of canopy reflectance model based correction.

In this study, a geometric-optical canopy reflectance model (Li and Strahler 1992) which includes calculations of canopy shadowing as a function of slope and aspect is used within an inversion framework to correct for the topographic effect on recorded spectral signals. This new topographic correction approach is described in the next section, and then evaluated two ways for a Rocky Mountain forest study area in western Canada. First, the actual digital values from uncorrected data are compared against five PE corrections, two SCS corrections and the MFM-TOPO PBM method with respect to the magnitude of topographically-induced variation that is removed. Second, land cover image classification results using the topographically corrected data from the various PE, SCS and the MFM-TOPO approaches are compared to uncorrected data with respect to individual forest class accuracy.

2. PBM correction using a canopy reflectance model: MFM-TOPO

The new canopy reflectance model-based topographic correction (MFM-TOPO) was developed based on the success of the canopy-based SCS and SCS+C corrections and other canopy reflectance model based BRDF corrections (Latifovic *et al.* 2003), and the availability of a suitable model (Li and Strahler 1992) and a flexible, indirect inversion capability (MFM) for its use (Peddle *et al.* 2000, 2003b, 2004). The Li and Strahler (1992) geometric optical mutual shadowing (GOMS) canopy reflectance model was selected for use in MFM-TOPO due to: (1) its computational efficiency and relative simplicity; (2) its ability to accurately characterize reflectance at scales ranging from forest stands to moderate and coarser spatial resolutions (Schaff *et al.* 1992, Li and Strahler 1992, Abuelgasim and Strahler 1994, Schaff and Strahler 1994); (3) its explicit inclusion of slope and aspect as model inputs; and (4) its performance relative to other models (Peddle *et al.* 1999).

The MFM-TOPO canopy reflectance model based correction involves three main steps: (a) parameterization and creation of look-up tables (LUTs) containing canopy structure, terrain orientation, view and illumination geometry, and modelled reflectance using the multiple-forward-mode (MFM) approach (Peddle *et al.* 2000, 2003b, 2004), (2) a LUT inversion procedure (Soenen *et al.* 2007) similar to that described by Kimes *et al.* (2000) to relate image spectral response to forest structure

and terrain geometry, and (3) a final MFM-LUT retrieval of canopy parameters and normalized terrain inputs to determine the final normalized reflectance value. These three stages are described below.

In the first stage, a set of MFM-LUTs is constructed that contains modelled reflectance values as potential solutions to the inversion problem, together with the structural and terrain (slope and aspect) parameters used as input to the model and associated with the forward-mode reflectance output. The MFM-LUTs are created through iterative MFM-GOMS model executions where a user-defined range of input structural and terrain parameters are varied by a set increment. The range and increment size can be set with no *a priori* information (Peddle *et al.* 2007), but are typically selected based on general observed structural conditions (Soenen *et al.* 2007). The illumination and viewing geometry at the time of image acquisition as well as the spectral (endemember) signatures for the dominant forest components (e.g. sunlit canopy, sunlit background, shadow) are known and held constant in all model runs. Alternatively, spectral signatures can be varied along with structure and terrain in the MFM process (e.g. for larger area applications and/or multi-temporal data sets) as it is not necessary to explicitly include these as constants for the dominant species. When available and appropriate, *a priori* knowledge of scene component signatures reduces MFM-LUT size and the number of potential solutions to the inversion problem and improves computational speed. The only requirement in specifying terrain parameters as input to MFM-TOPO is that flat terrain must be included in the range of MFM slopes and aspects for use in stage 3, since that is required in the final terrain correction.

In the second stage, a distribution of potential reflectance matches is selected from the modelled output using MFM-LUT based indirect inversion (Kimes *et al.* 2000, Soenen *et al.* 2007). The indirect inversion procedure requires an image input and a set of modelled reflectance values describing the complete range of potential structural and terrain conditions within the image. The procedure operates by matching reflectance values from a given image pixel with reflectance values from the modeled reflectance values resident in the MFM-LUT. The spectral, structural, illumination, view, and terrain values associated with the reflectance value from the model that matches with the remotely sensed image reflectance value are output for use in the third stage. Reflectance matches are selected from the modelled output if: (1) the modelled reflectance values in n-dimensional spectral space are within a limit defined by a root-mean-square-error tolerance derived using measured (i.e. airborne or satellite) and modelled (MFM-LUT) reflectance; and (2) the terrain inputs to the modelled reflectance match the terrain values derived from a digital elevation model (DEM) co-registered to the image. Each of the matches contains the MFM-LUT canopy structure and terrain input parameters that yielded the matching reflectance. The matches represent potential solutions to the inversion problem. If the solution set is non-unique, then a set of rules (Soenen *et al.* 2007) is invoked to limit the potential matches to a single set of structural input parameters for use in the third processing stage. In MFM-TOPO, the median structural values within the distribution of potential matches are selected in these cases.

In the third and final stage, the actual terrain correction is performed as a function of the modelled canopy structure for a given pixel. The set of canopy structural parameters determined from stage 2 for the sloped pixel (in this case, from MFM-GOMS: density, horizontal and vertical crown radius, height to crown centre, height distribution) is used as a search key to access in the MFM-LUT the

corresponding entry possessing the same canopy structure, but having flat terrain instead. The correction is based on four fundamental capabilities: (1) the GOMS model includes terrain slope and aspect as model inputs, and thus the reflectance output by the model is a function of terrain geometry; (2) when run in MFM, the full range of slopes (flat to steep) and aspects are captured in the MFM-LUT, with each LUT entry possessing a slope and aspect value, a set of structural values, and an output (modelled) reflectance value; (3) for a given pixel, the MFM inversion results from stage 2 provides the structural parameters for the sloped pixel; and (4) the identical set of structural conditions exists in the MFM-LUT for the flat terrain case, with an associated reflectance value. This reflectance value for flat terrain is the MFM-TOPO terrain corrected output reflectance value. Thus, the topographically normalized modelled reflectance for a given sloped pixel is simply the MFM modelled reflectance value for those same structural conditions on flat terrain. There will always be one unique match since the MFM-LUT contains the full range of all structural inputs for both flat and sloped terrain. Thus, the ''MFM-LUT cross-reference'' to achieve the topographic correction from sloped to flat terrain is ensured. This part of MFM-TOPO is similar in concept to an earlier algorithm designed for topographic correction of spectral mixture analysis scene fractions (Johnson *et al.* 2000). In MFM-TOPO, since the MFM-LUT already contains reflectance values for flat and sloped terrain, no additional forward-mode model runs are required, thus the total computational time remains a function of MFM-LUT size and search algorithm speed. We also note that reflectance values for any terrain orientation could be obtained for a given forest stand pixel (e.g. instead of retrieving a reflectance output for flat terrain, this could be done for any specified slope and aspect, such as simulating a 20° slope from a 45° slope, or, conversely, forest stand pixels on flat terrain could be simulated in terms of their corresponding reflectance on steeper slopes and different aspects).

3. Experimental design

Two experiments were performed to assess MFM-TOPO against a variety of other PE and SCS topographic correction methods. In the first experiment, the reflectance values derived from each correction were assessed statistically with respect to the original (uncorrected) reflectance values and the pixel terrain orientation. The second experiment involved nine separate mountain terrain landcover classifications using a different input dataset in each case (uncorrected data, and from the 5 PE, 2 SCS corrections and MFM-TOPO), with the comparison based on the classification accuracies obtained.

3.1 *Study area and dataset*

The study area is located in the front range of the Canadian Rocky Mountains in Kananaskis Country, Alberta, Canada (51.02° N, 115.07° W). The area covers approximately 1600 km^2 and includes a full range of terrain aspects, and slopes ranging from 0 to 50°. The area is dominated by stands of Lodgepole pine (*Pinus contorta* Dougl.), with intermittent stands of Trembling Aspen (*Populus tremuloides* Michx.), White spruce (*Picea glauca* (Moench) Voss), and Englemenn spruce (*Picea engelmannii* Parry ex Engelm.). Typical measured stem density for the area ranged from 700 to 3000 stems/ha in conifer stands and 700–2000 stems/ha in deciduous stands. Mean stand height ranged from 10 to 19 m.

Satellite imagery was acquired over the study area by the Système Pour l'Observation de la Terre (SPOT-5) HRVIR sensor on August 12, 2004 with a spatial resolution of 10 m. A DEM at 25 m spatial resolution was subsequently co-registered to the imagery with sub-pixel accuracy (geometric RMS error=4.9 m). The SPOT data were converted to reflectance using published gain values and a correction for atmospheric effects using the empirical line method (Smith and Milton 1999). The image data were resampled to 25 m spatial resolution prior to topographic correction and subsequent classification procedures.

A series of field spectra were acquired near the time of SPOT overpass (nominal 10:30 a.m. local time) between July 15 and August 27, 2004. Endmember spectra for sunlit canopy, background and shadow were collected using an Analytical Spectral Devices full range (ASD FR: 350–2500 nm) portable field spectroradiometer following protocols developed by Peddle (1998) and Peddle *et al.* (2001) and used to parameterize the spectral inputs to the canopy reflectance model. It should be noted that measured spectra are an optional requirement of MFM since, if these are not available or desired, then the first stage of the MFM-TOPO correction process can instead simply use a spectral range. MFM does not require field inputs.

Other model inputs consisted of ranges of structural and terrain values, as well as the solar illumination and satellite viewing geometry at the time of SPOT image acquisition (table 1). The values that were varied were set to ensure a comprehensive range of values were included in the MFM-LUTs, however, as above, we note that no *a priori* information is required and in fact the MFM-TOPO procedure can be used in situations where little or no information about structure or terrain of a given area is known (Peddle *et al.* 2007).

3.2 *Assessing terrain normalized reflectance*

Prior to image classification it was possible to assess the corrections by examining the relationship between the recorded signal and terrain orientation. If forest stands of similar species type and structure are observed over varying terrain orientation they will show a trend of decreasing brightness with increasing angle of incidence (Soenen *et al.* 2005). This effect is increasingly prevalent at longer wavelengths. To test this, a subset of pixels covering forest stands of equivalent structure over a range of terrain orientations was selected. The brightness (DN) values for the uncorrected and topographically corrected pixels were compared statistically against their

Table 1. Structural and geometric parameter ranges and increments used in the MFM algorithm for look-up table generation.

Model Parameter	Minimum	Maximum	Increment
Density (trees m^{-2})	0.05	0.5	0.05
Horizontal Crown Radius (m)	0.5	6.5	1
Vertical Crown Radius (m)	0.5	6.5	2
Height to Crown Center (m)	4	14	2
Height Distribution (m)	5	25	5
Slope (°)	0	60	5
Aspect (°)	0	345	15
Solar Zenith Angle (°)	37	37	constant
Solar Azimuth Angle (°)	157	157	constant
View Zenith Angle (°)	7	7	constant
View Azimuth Angle (°)	15	15	constant

corresponding cos (*i*). The premise of this test was that any signal variance in the corrected imagery should be explained by stand structure, not topography.

3.3 *Classification procedure*

A series of supervised maximum likelihood classifications was performed for the uncorrected and the various topographically corrected image datasets. The latter included imagery corrected using the cosine, *C*-correction, Minnaert, statistical empirical, *b*-correction, SCS, SCS + C, and the new MFM-TOPO canopy reflectance model method. Four dominant alpine and sub-alpine forest classes were identified (pine, spruce, deciduous, mixed) from the Alberta Vegetation Inventory (AVI, 1991) and from supporting field observations. Additional non-forested classes of exposed rock, water, grassland/shrub, and roads were included to ensure a full and proper characterization of all land cover in the region. Training data for the maximum likelihood classifications were taken from the AVI and with reference to field information. A separate, independent, mutually exclusive set of validation pixels was also extracted from the AVI for classification accuracy assessment. Training and validation pixels were obtained randomly from within the inventory polygons according to dominant overstory species type and area. The same set of training and validation pixel locations was used for all classifications of the original uncorrected image and the various corrected images, to ensure experimental consistency for comparisons.

The classification results were evaluated across a series of incidence angle ranges to isolate and further assess the effect of topography (and its correction) on classification accuracy. Incidence angle and the cosine of the incidence angle (cos(*i*)) serve as well-known and fundamental terrain parameters (Teillet *et al.* 1982, Soenen *et al.* 2005) and have been used in past classification testing (Meyer *et al.* 1993). In this study area, the values for cos(*i*) for vegetated slopes ranged from 0 to 1, corresponding to terrain oriented away from and facing towards the source of illumination, respectively. As an example, for solar illumination conditions found in this study (37° solar zenith angle and 157° solar azimuth angle at the time of SPOT image acquisition), flat terrain would have a cos(*i*) value near 0.79. A 30° slope at 320° aspect would have a cos(*i*) value near 0.40 while a 30° slope at 160° aspect would have a cos(*i*) value near 0.99. Validation pixels obtained at random from each dominant species group within the AVI were grouped according to the distribution of terrain orientation expressed by cos(*i*). The area within the study site selected for validation within each group was proportional to its representation within the group (table 2). A series of accuracy assessments was created for each species within each

Table 2. Summary of validation pixel area within the Kananaskis study area as a function of surface terrain and illumination angle, expressed as cosine of incidence [cos(*i*)].

Cosine of Incidence	Validation Pixel Area (ha)			
	Pine	Spruce	Deciduous	Mixed
0 to 0.1	2.96	11.16	–	–
0.1 to 0.2	15.68	62.44	–	–
0.2 to 0.3	101.84	250.56	1.23	2.53
0.3 to 0.4	472.88	764.60	2.54	3.96
0.4 to 0.5	1492.00	1569.96	19.16	9.96
0.5 to 0.6	3254.56	2369.52	40.00	28.76

terrain orientation group. The relative effectiveness of a topographic correction was assessed with respect to the improvements in classification accuracy compared to that obtained from the uncorrected data.

4. Results

4.1 *Terrain normalized reflectance results*

There were moderate positive linear relationships between terrain orientation ($\cos(i)$) and uncorrected DN in SPOT band 1 ($r^2=0.44$), band 2 ($r^2=0.38$), band 3 ($r^2=0.56$), and band 4 ($r^2=0.52$). The strength and trend of these relationships were consistent with the range reported in other studies for image channels covering similar wavelengths (Teillet *et al.* 1982, Meyer *et al.* 1993, Vincini and Frazzi 2003). The difference in uncorrected observed signal from stands of similar structure on shaded and sunlit slopes was 60 DN (figure 1). It was clear from even a cursory

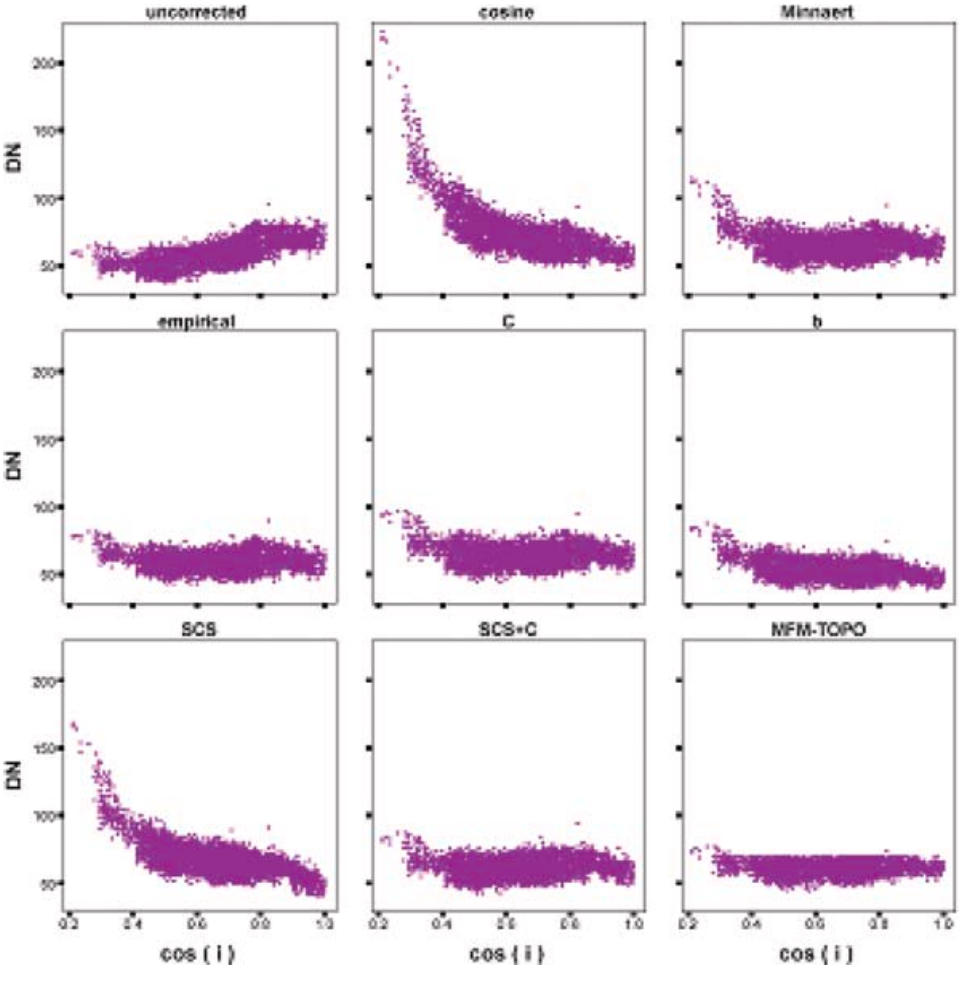

Figure 1. Assessment of radiometric response and topography for corrected and uncorrected SPOT band 3. Digital number is plotted against cosine of the incidence angle. Points represent pixels within medium to high density pine stands as classified by the Alberta Vegetation Inventory (AVI).

observation that a number of the correction methods (e.g. cosine, SCS) did not remove the influence of terrain on recorded signals for all terrain orientations and in some cases even introduced additional and new substantial errors (figure 1). The cosine correction, for example, had a difference of 191 DN between shaded and sunlit terrain, exceeding the difference in the uncorrected data. In this instance, any connection between the physical-structural conditions of the forest stands and the reflected radiance has been lost as a result of an erroneous correction.

The statistical-empirical, C, Minneart and SCS+C corrections all reduced the topographic effect to a similar extent. These corrections reduced the slope of the linear relationship (e.g. SPOT band 3 uncorrected data=41, statistical-empirical=0, $C=-0.4$, SCS+C=5.6) found between the uncorrected data and $\cos(i)$ while preserving the observed variance. However, while these corrections appeared to be more effective at reducing the slope of the linear relationship, they still had an overcorrection feature for shaded slopes [$<0.4\cos(i)$] similar in trend to the SCS and the cosine correction, though with a lesser magnitude. The b correction results showed similarities to the C and SCS+C corrections for shaded slopes and had a slight overcorrection for sunlit slopes (>0.8).

The MFM-TOPO correction showed a near complete removal of the relationship between topography and spectral response (DN). The MFM-TOPO correction also appeared to be effective at $\cos(i)<0.4$, unlike the PE methods. A threshold effect is apparent, however, where there is a concentration of DN=70 values, with few values above. This effect is likely to be a result of the inversion procedure. Since median structural values are selected from the distribution of solutions, it is likely that more extreme structural cases may be underrepresented in the inversion output, resulting in lower DN variance in corrected imagery. Results similar to those found in figure 1 were found for other bands (not shown). The utility of these corrections is further explored in the following terrain classification application.

4.2 *Classification accuracy results*

Classification accuracy was used to assess the relative effectiveness of each topographic correction. A proper topographic correction should remove any signal variance as a result of terrain orientation and should simplify the connection between the natural physical-structural state of the stand and the spectral signal received at the sensor. Classification of forest cover type in mountainous areas can be compromised due to the high amount of spectral overlap within and between classes induced considerably by terrain influence and not fully by actual cover change and variability (figure 2). A topographic correction should remove any shading or brightening effects as a result of terrain that increases the level of within-class variance and leads to this overlap and subsequent classification error. Thus, a classification algorithm should be able to assign corrected pixels to the different forest cover types more effectively.

The uncorrected classified data showed low levels of classification agreement with the validation data for Lodgepole pine (figure 3) on topographically shaded slopes ($\cos(i)=0$–0.3). Most of these topographically shaded pine slopes were incorrectly classified as spruce. As $\cos(i)$ increased, the level of agreement between classified and validation pixels increased. The trend for spruce was opposite (figure 4), with agreement decreasing with $\cos(i)$. Over less sloped terrain ($\cos(i)=0.4$–0.6) nearly half of the validation pixels were incorrectly classified as pine. The deciduous (figure 5) and mixed stands (figure 6) on slopes with higher angles of incidence

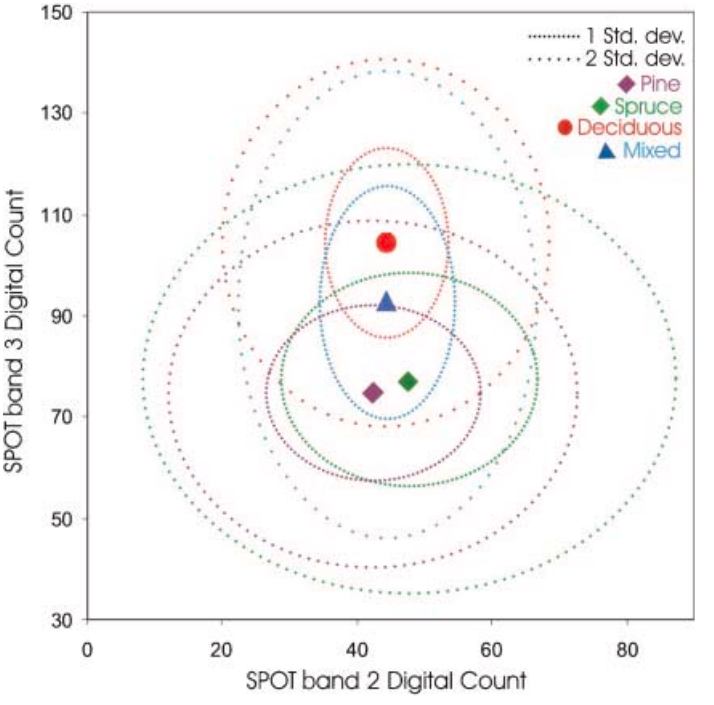

Figure 2. Distribution for uncorrected training pixels within two-dimensional spectral space for SPOT bands 2, 3 for the four forest classes. The positions of one and two standard deviations about the mean are shown for each class distribution. The probability density function for the maximum likelihood classification is derived from these distributions.

($\cos(i)=0.2$–0.5) were misclassified as both spruce and pine. The amount of correctly classified pixels increased with $\cos(i)$.

There were small increases in producer accuracy (pixels correctly classified as a given class divided by the number of validation pixels for that class) for pine and deciduous classes taken from the cosine corrected data compared to the uncorrected data (table 3). These increases were less than the increases in accuracy achieved by using any other correction method for shaded slopes ($\cos(i)<0.4$). Over less sloped terrain, the cosine corrected data had a greater increase in producer accuracy than over highly sloped terrain. The accuracy for the cosine corrected data was also higher than accuracy for most other corrections over less sloped terrain ($\cos(i)>0.4$). These results were in agreement with those from a previous study which found that the cosine correction was most effective over low slope angles and increasingly ineffective as $\cos(i)$ approached 0 (Soenen *et al.* 2005).

Trends in classification accuracy similar to those described for from the cosine corrected data were observed for most other correction methods (*b*, Minneart, SCS and SCS+C) with the exception of the statistical empirical and MFM-TOPO methods. The statistical empirical and MFM-TOPO corrected data maintained higher levels of pine and deciduous producer accuracy relative to the other corrected and uncorrected data across the entire $\cos(i)$ range (figures 3 and 5). The results from the statistical empirical corrected data agree with those from a previous study which found that it was effective across a wide range of slope-aspect combinations (Soenen *et al.* 2005). The *C* corrected data also maintained higher levels of accuracy in the

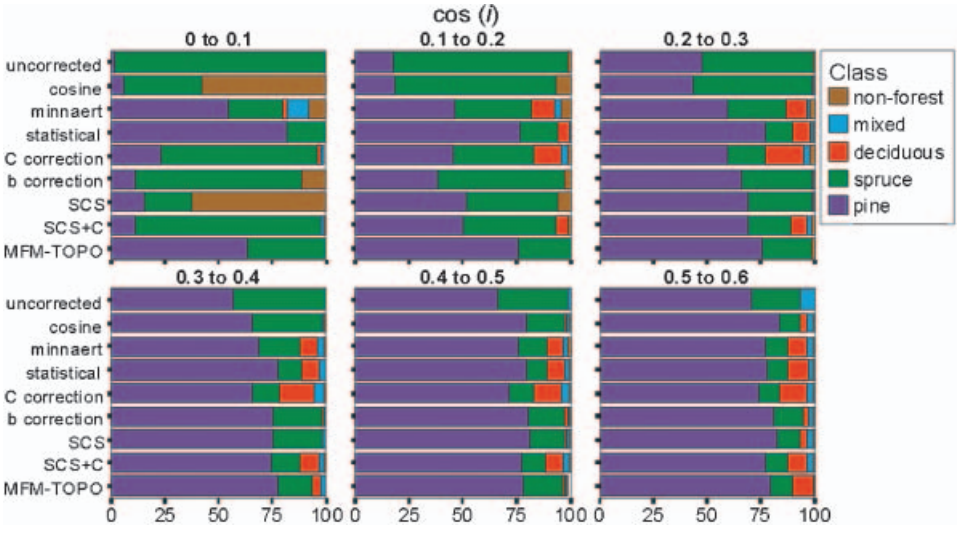

Figure 3. Classification results for pine stands over a number terrain orientations (cosine of incidence 0–0.6 in 0.1 increments). Bars indicate the percentage of pine validation pixels classified to each vegetation class (classes other than pine represent errors of omission). Producer's accuracy for pine is indicated by leftmost bar, unless absent (i.e. pine accuracy=0%). Remaining incorrectly classified validation pixels displayed as bars to right of pine class. Bars sum to 100%. Non-forest class results aggregated for illustration here.

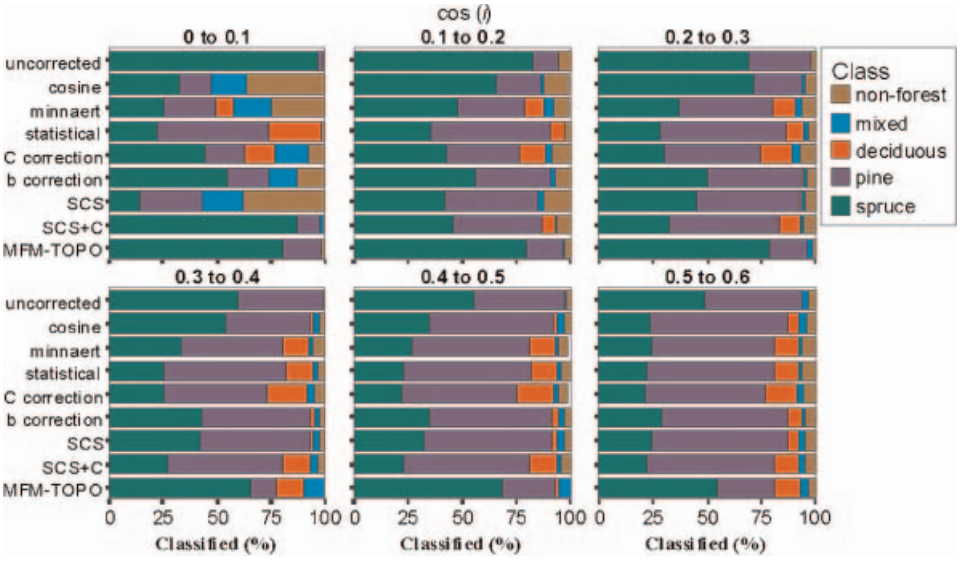

Figure 4. Classification results for spruce stands over a number terrain orientations (cosine of incidence 0–0.6 in 0.1 increments). Bars indicate the percentage of spruce validation pixels classified to each vegetation class (classes other than spruce represent errors of omission). Producer's accuracy for spruce is indicated by leftmost bar unless absent (i.e. spruce accuracy=0%). Remaining incorrectly classified validation pixels displayed as bars to the right of spruce class. Bars sum to 100%. Non-forest class results aggregated for illustration here.

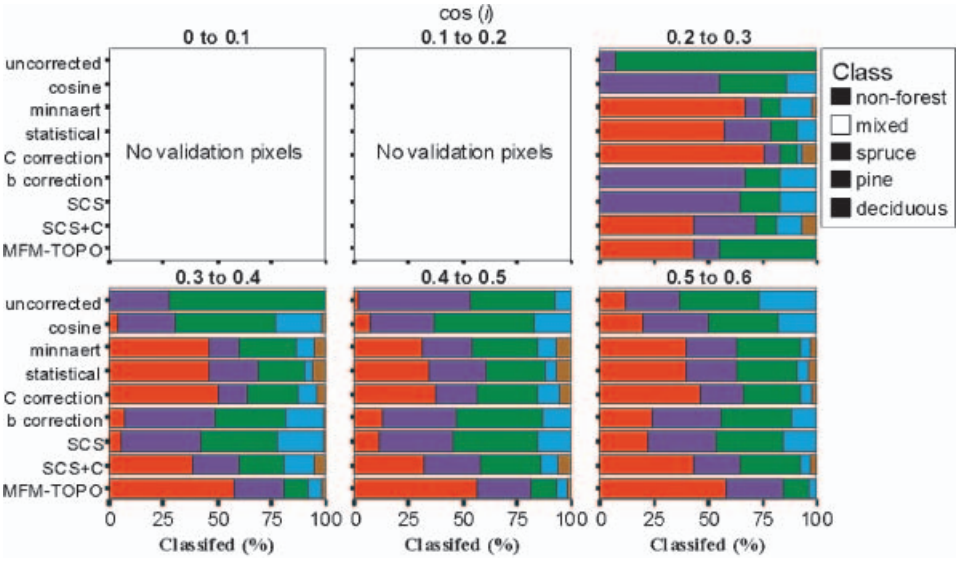

Figure 5. Classification results for deciduous (Trembling Aspen) stands over a number of terrain orientations (cosine of incidence 0–0.6 in 0.1 increments). Bars indicate the percentage of deciduous validation pixels classified to each vegetation class (classes other than deciduous represent errors of omission). Producer's accuracy for deciduous forest is indicated by leftmost bar unless absent (i.e. deciduous accuracy=0%). Remaining incorrectly classified validation pixels displayed as bars to the right of deciduous class. Bars sum to 100%. There were no deciduous validation pixels present in areas where cos(i)<0.2. Non-forest class results aggregated for illustration here.

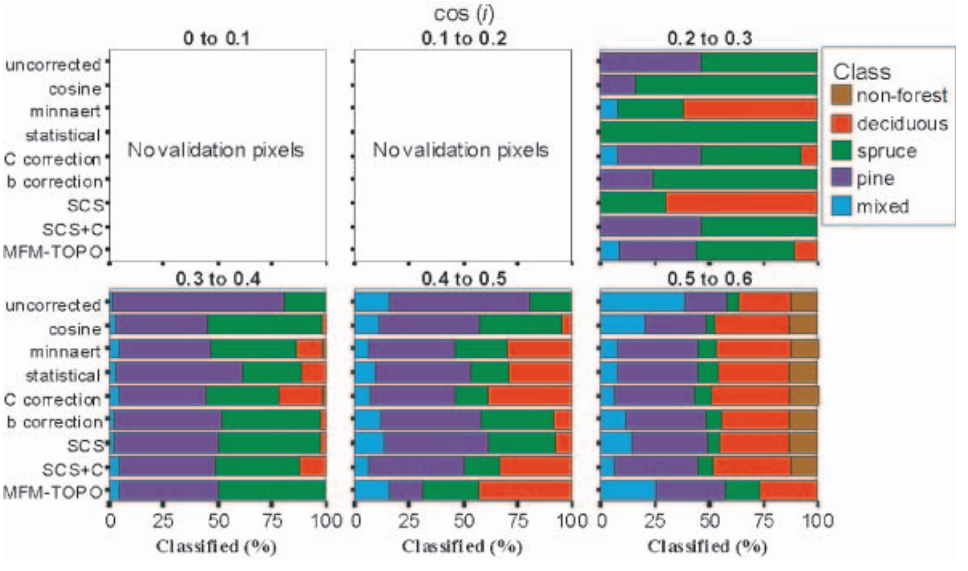

Figure 6. Classification results for mixed (deciduous/coniferous) stands over a number of terrain orientations (cosine of incidence 0–0.6 in 0.1 increments). Bars indicate the percentage of mixed validation pixels classified to each vegetation class (classes other than mixed represent errors of omission). Producer's accuracy for mixed forest is indicated by leftmost bar unless absent (i.e. mixed forest accuracy=0%). Remaining incorrectly classified validation pixels displayed as bars to the right of mixed forest class. Bars sum to 100%. There were no validation pixels in areas where cos(i)<0.2. Non-forest class results aggregated for illustration here.

Table 3. Individual producer accuracy for the uncorrected data, and the eight topographic correction methods tested. Results for the four forest classes of interest are grouped by terrain categories of cosine of incidence angle [cos(*i*)]. Average accuracy is the average of producer accuracy from 0 to 0.6 cos(*i*). Overall accuracy and Kappa for the full range of terrain orientations (i.e. 0>cos(*i*)<1) is also included.

		Topographic Correction Method								
cos(i)	Species	uncorr.	cosine	Minn.	C	stat.	b	SCS	SCS+C	MFM
0 to 0.1	pine	1	5	54	23	81	11	15	11	63
	spruce	97	32	25	45	22	55	14	56	81
	decidous	–	–	–	–	–	–	–	–	–
	mixed	–	–	–	–	–	–	–	–	–
0.1 to 0.2	pine	17	18	46	46	77	38	52	51	75
	spruce	83	66	47	43	35	57	42	46	79
	decidous	–	–	–	–	–	–	–	–	–
	mixed	–	–	–	–	–	–	–	–	–
0.2 to 0.3	pine	47	43	60	60	77	66	69	69	75
	spruce	70	71	38	30	28	50	45	32	79
	decidous	0	0	67	76	57	0	0	43	42
	mixed	0	0	8	8	0	0	0	0	8
0.3 to 0.4	pine	57	65	69	65	77	75	75	74	78
	spruce	59	54	33	26	26	43	42	27	65
	decidous	0	3	46	50	46	7	5	38	58
	mixed	1	3	5	4	3	2	2	5	5
0.4 to 0.5	pine	66	80	75	72	80	81	81	78	78
	spruce	55	35	27	22	23	35	32	23	68
	decidous	1	7	31	38	34	13	11	32	57
	mixed	16	11	6	7	9	12	13	6	16
0.5 to 0.6	pine	71	83	77	74	78	81	83	78	79
	spruce	49	23	24	21	22	29	24	22	54
	decidous	12	20	40	46	40	23	22	42	58
	mixed	39	20	8	6	8	11	14	6	25
Average 0 to 0.6	pine	43	49	63	57	78	59	63	60	75
	spruce	69	47	32	31	26	45	33	34	71
	decidous	3	7	46	53	44	11	10	39	54
	mixed	14	9	7	6	5	6	7	4	14
entire range	OVERALL	64.15	61.73	56.77	53.55	56.60	61.84	60.80	57.20	69.32
	Kappa	0.44	0.40	0.36	0.33	0.35	0.40	0.39	0.35	0.49

deciduous class relative to the other correction methods. The *b*-correction results showed smaller increases in producer accuracy for pine when compared to the other empirical approaches (figure 3). This is likely due to the strong linear (as opposed to log-linear) trend found in the relationship between shorter wavelengths and terrain orientation. The highest average producer accuracy for the pine class was achieved with the statistical empirical (78%) and MFM-TOPO corrected (75%) data (table 3). The highest average accuracy for the deciduous class was achieved using the MFM-TOPO corrected data (54%) followed by the *C*-correction and statistical empirical corrected data.

The MFM-TOPO corrected data also yielded higher accuracy relative to other correction methods for the spruce class (figure 4). The producer accuracy for the

spruce class observed for all other corrected data was less than that of the uncorrected data (table 3). The accuracy also decreased with increasing cos(*i*) for all correction methods. As cos(*i*) increased, the validation pixels were increasingly misclassified as pine. On the most shaded slopes (cos(*i*) 0–0.1) the level of producer accuracy for pine stands increased, compared to classification results using the uncorrected data, with MFM-TOPO having the highest increase (+62%), and followed by the SCS+C correction (+9%). With both, the accuracy for spruce stands remained relatively high (MFM-TOPO: 80.8%, SCS+C 56.5%). As cosine of incidence increased, the MFM-TOPO corrected data continued to achieve relatively high producer accuracy for both pine and spruce stands (figures 3 and 4). Overall accuracy, for the entire range of terrain orientations, was also improved using the MFM-TOPO correction (table 3).

None of the corrections were effective at increasing producer accuracy for the mixed class compared to that observed in the uncorrected classification for cos(*i*) 0.4–0.6 (table 3). Over steeper slopes (cos(*i*)<0.4) the MFM-TOPO, *C*, and Minnaert corrected data yielded slight improvements. The majority of mixed forest validation pixels were misclassified as pine or spruce at cos(*i*) 0.2–0.3, with the exception of the SCS and Minneart corrected data, for which the mixed class was misclassified as deciduous. The majority of mixed forest class validation pixels at cos(*i*) 0.4–0.6 were misclassified as pine or deciduous. The low mixed forest class accuracies are likely due to the nature of this type of class that is often highly variable, non-Gaussian, and possibly multi-modal. These types of class distributions may be expected to violate the assumption of normality in the maximum likelihood classifier, and therefore would not be characterized properly by measures of central tendency. Improved mixed forest class accuracies would likely require a refined or multiple mixed forest class set, or the use of a non-parametric classifier.

5. Discussion

5.1 *Perspectives on classification results*

Using original, uncorrected data, the general misclassification of deciduous and pine species in shaded terrain was likely a result of two primary factors: (1) shaded area accounted for only a small percentage of the total scene and thus, these areas were under-represented when randomly selecting training pixels from the image; and (2) the increase in shadowing forced the shaded pixels into spectral space where the probability density for the spruce class was high (figure 2). As a result, the majority of the pixels dominated by pine in shaded areas were classified as spruce, with the deciduous and mixed stands classified primarily as pine or spruce.

With a PE correction, spruce and pine reflectance was shifted identically and had a similar radiometric response. In reality, these two types of stands on flat terrain would be shaded differently due to differences in physical structure (figure 7). Lodgepole pine canopy tends to have less vertical density and be more discontinuous, while spruce is the structural opposite. As a result, stands of spruce on flat terrain maintain a higher level of shadow and as a result have a lower radiometric signal for green and near infrared bands (figure 7). The classification results for the PE corrections showed a decrease in classification agreement for spruce as the level of agreement increased for pine stands. This may indicate that the PE corrections are too general and do not increase the level of spectral separability between the pine and spruce normalized pixels.

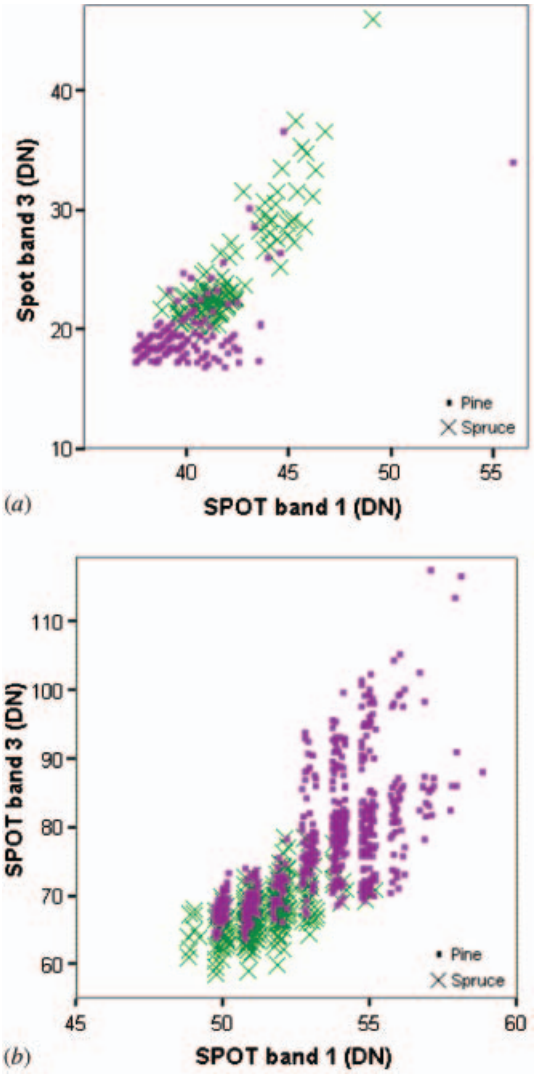

Figure 7. A random selection of pixels from SPOT imagery dominated by pine (n=400) and spruce (n=350) stands on (*a*) sloped, shaded terrain (cos (i)<0.2) and (*b*) flat terrain (<8° slope).

The average producer accuracy over the range of cos(i) resulting from the MFM-TOPO corrected data, however, was high for both spruce (71%) and pine (75%). This suggests that the MFM-TOPO correction increases separability between pine and spruce classes for normalized pixels. The inherent structural framework embedded in the MFM-TOPO method likely provides an advantage when normalizing imagery of forested areas where spectral response is dependant not only on the vegetation spectral properties, but also on the physical structure of the canopy.

5.2 *Perspectives on MFM-TOPO*

The canopy reflectance model based MFM-TOPO correction is possible as a result of efficient and effective canopy reflectance model inversion procedures (Kimes *et al.*

2000, Peddle *et al.* 2004, Soenen *et al.* 2007). While these procedures are becoming increasingly robust there are also several issues that warrant attention. One important issue associated with the type of indirect inversion utilized in MFM-TOPO is that the inversion problem is ill-posed with respect to the requirement for a unique solution (Combal *et al.* 2002). Since the inversion may have multiple solutions it is necessary to invoke a set of rules to select the most likely solution (Soenen *et al.* 2007). However, that solution still has the potential to be erroneous or less than optimal and may therefore cause improper or less than ideal pixel correction. This may manifest as a threshold where more extreme structural cases, and thus high or low reflectance values, may be under-represented in the topographic correction output (figure 1). However, minor errors in structural prediction resulting from the use of a median measure of central tendency should not introduce significant error into the resulting normalized reflectance. The higher class accuracies across all species obtained using the MFM-based correction support this.

It is important to note, however, that a unique solution is not always desired, required, or in some cases, possible. For example, ranges of solutions can be fully appropriate and informative in a variety of applications in forestry, inventory, as well as for modelling productivity, hydrology, eco-physiology and carbon budget estimates. The reporting of output ranges may also be more appropriate and indicative of the actual level of information content extraction possible, even from the most sophisticated model and inversion schemes.

There is also currently a need to use accurate spectra for the primary scene components including overstory species, understory species and shadowed vegetation. To achieve accurate model inversion, these reference endmember spectra should be collected under conditions similar to the time of image acquisition, unless the spatial resolution of the image data is sufficiently high to permit use of image endmembers. Canopy reflectance models have also been used to create selected endmember reflectance inputs (Hall *et al.* 1995, Peddle *et al.* 1999). If, however, no endmember spectra are available or feasible, for whatever reason, it is still possible within the MFM-LUT creation stage to input a range of input spectra values. This would also allow use of generalized or library spectra with an associated variance to account for temporal, atmospheric, and illumination differences. Although a powerful capability, one potential drawback may be compounding the ill-posed inversion problem by introducing additional dimensionality to the solution set space.

One of the core advantages of a canopy reflectance model based approach is the ability to explicitly account for a full variety of the main environmental, geometrical, structural, illumination, edaphic, morphometric and ecological factors that influence airborne and satellite image spectral response (Hall *et al.* 1997, Peddle *et al.* 1999). This is of particular importance over large areas where multiple scene acquisitions are required, each with possibly different view, solar and terrain geometries that can nonetheless be dealt with explicitly in this modeling context (e.g. Peddle *et al.* 2004). In essence, by treating these factors as sources of refined information within a systems based approach, instead of regarding them as noise to be either ignored or suppressed, a more appropriate and robust radiometric image processing framework is created while still maintaining a manageable set of model inputs which, in the MFM inversion context, is fully flexible and unconstrained to the user since location specific information is not required. This allows the full

power of sophisticated modelling to be accessible over large areas and for diverse imaging, terrain and information content applications and needs. This satisfies a key requirement of many global change research programmes that involve a great diversity of ecosystems to be considered over different parts of the Earth using multi-temporal imagery from a variety of sensors with different properties. As evidence of this, we note that MFM has also been used successfully for a variety of other forest information needs, such as estimation of biomass, LAI, forest classification (both supervised and also unsupervised cluster labelling) stand volume, and structural change detection (e.g. Pilger *et al.* 2003, Peddle *et al.* 2000, 2003b, 2003c, 2004, 2007).

6. Conclusion

In this paper we have demonstrated both theoretically and empirically the advantages of using a canopy reflectance model based approach for topographic correction in forested terrain. Image data corrected using the MFM-TOPO method showed improved treatment of topographically induced image reflectance variation and subsequently, classifications showed higher levels of agreement with validation data compared with image data corrected using a variety of other PE and SCS topographic correction methods. Thus, the MFM-TOPO correction method is potentially a more appropriate topographic correction in forested areas since it more accurately characterizes the relationship between topographic orientation, forest stand structure and radiometric response. MFM-TOPO accounts for the topographic effect as a sub-pixel scale phenomenon driven by changes in the orientation of individual tree crowns within the canopy which in turn affects the fundamental sub-pixel components: sunlit canopy, sunlit understory, and shadow. It represents the preferred way to implement topographic correction within the SCS framework. Other photometric and empirical correction methods treat the topographic effect as a pixel level phenomenon (i.e. sun-terrain-sensor, and not at sub-pixel scales) and without regard for important forest structural influences, and thus those corrections are overly generalized and not representative of the topographic effect in forested scenes. While other correction methods do improve agreement for some dominant classes it is at the cost of agreement in other classes with high spectral similarity. For example, the cosine, Minnaert, and statistical empirical corrections improved the producer accuracy of the pine class at cos(i) 0–0.1, but had decreased accuracy in the spruce class.

The improved topographic correction methods presented here are useful in a variety of applications ranging from forestry, climate change research, watershed and basin hydrology analyses, geomorphology and geomorphometry, among others. Accordingly, it is recommended that consideration be given to canopy reflectance model based corrections in forested areas, particularly given the other forest information that can be obtained from MFM inversion in a coupled modelling context, such as biomass, LAI, land cover classification, stand volume, and structural change, while also being well suited to larger area and global datasets and applications.

Acknowledgements

This research was supported in part by grants to Dr. Peddle and collaboration from the Natural Sciences and Engineering Research Council of Canada (NSERC), Alberta Ingenuity Centre for Water Research (AICWR), Prairie Adaptation

Research Collaborative (PARC), Water Institute for Semiarid Ecosystems (WISE), Natural Resources Canada, NASA Goddard Space Flight Centre/University of Maryland, Alberta Research Excellence Program, Miistakis Institute of the Rockies (DEM), Center for Remote Sensing, Boston University (GOMS model) and the University of Lethbridge. Computing resources were provided through the Western Canada Research Grid (WestGrid NETERA c3.ca). SPOT imagery was acquired from Iunctus Geomatics Corporation and the Alberta Terrestrial Imaging Centre (ATIC), both of Lethbridge Alberta. We are grateful to Sam Lieff, Adam Minke and Kristin Yaehne for field assistance and the staff at the Kananaskis Field Stations for logistical support in the field.

References

AVI, 1991, Alberta vegetation inventory standards manual version 2.1. Alberta Environmental Protection, Resource Data Division, Data Acquisition Branch, Edmonton, AB, Canada.

ABUELGASIM, A.A. and STRAHLER, A.H., 1994, Modeling Bidirectional Radiance Measurements Collected by the Advanced Solid-State Array Spectroradiometer (ASAS) over Oregon Transect Conifer Forests. *Remote Sensing of Environment*, **47**, pp. 261–275.

CAVAYAS, F. and TEILLET, P.M., 1985, Geometric model simulations of conifer canopy reflectance. In *Proceedings of the 3rd International Colloquium on Spectral Signatures of Objects in Remote Sensing*, 16–20 December 1985, Les Arcs, France, pp. 183–189.

CHEN, J.M., LI, X., NILSON, T. and STRAHLER, A., 2000, Recent advances in geometrical optical modelling and its applications. *Remote Sensing Reviews*, **18**, pp. 227–262.

COMBAL, B., BARET, F., WEISS, M., TUBUIL, A., MACE D., PRAGNERE, A., MYENI, R., KNYAZIKHIN, Y. and WANG, L., 2002, Retrieval of canopy biophysical variables from bidirectional reflectance using prior information to solve the ill-posed inverse problem. *Remote Sensing of Environment*, **84**, pp. 1–15.

GEMMELL, F., 1995, Effects of forest cover, terrain, and scale on timber volume estimation with thematic mapper data in a Rocky Mountain site. *Remote Sensing of Environment*, **51**, pp. 291–305.

GEMMELL, F., 1998, An investigation of terrain effects on the inversion of a forest reflectance model. *Remote Sensing of Environment*, **65**, pp. 155–169.

GU, D. and GILLESPIE, A., 1998, Topographic normalization of Landsat TM images of forests based on subpixel Sun-Canopy-Sensor geometry. *Remote Sensing of Environment*, **64**, pp. 166–175.

GU, D., GILLESPIE, A.R., ADAMS, J.B. and WEEKS, R., 1999, A statistical approach for topographic correction of satellite images by using spatial context information. *IEEE Transactions on Geoscience and Remote Sensing*, **37**, pp. 236–246.

HALL, F.G., KNAPP, D.E. and HUEMMERICH, K.F., 1997, Physically based classification and satellite mapping of biophysical characteristics in the southern boreal forest. *Journal of Geophysical Research*, BOREAS Special Issue, **102**, pp. 29567–29580.

HALL, F.G., SHIMABUKURO, Y.E. and HUEMMRICH, K.F., 1995, Remote sensing of forest biophysical structure in boreal stands of *Picea mariana* using mixture decomposition and geometric reflectance models. *Ecological Applications*, **5**, pp. 993–1013.

ITTEN, K.I. and MEYER, P., 1992, Geometric and radiometric correction of TM data of mountainous forested areas. *IEEE Transactions on Geoscience and Remote Sensing*, **31**, pp. 764–770.

JOHNSON, R.L., PEDDLE, D.R. and HALL, R.J., 2000, A model based subpixel scale mountain terrain normalization algorithm for improved LAI estimation from airborne CASI imagery. In *Proceedings, 22nd Canadian Symposium on Remote Sensing*, 21–25 August 2000, Victoria, BC, Canada, pp. 415–424.

JUSTICE, C.O., WHARTON, S.E. and HOLBEN, B.N., 1981, Application of digital terrain data to quantify and reduce the topographic effect on Landsat data. *International Journal of Remote Sensing*, **2**, pp. 213–230.

KIMES, D.S., KNYAZIKHIN, Y., PRIVETTE, J.L., ABUELGASIM, A.A. and GAO, F., 2000, Inversion methods for physically-based models. *Remote Sensing Reviews*, **18**, pp. 381–439.

LATIFOVIC, R., CIHLAR, J. and CHEN, J., 2003, A comparison of BRDF models for the normalization of satellite optical data to a standard Sun-Target-Sensor geometry. *IEEE Transactions on Geoscience and Remote Sensing*, **41**, pp. 1889–1898.

LI, X. and STRAHLER, A.H., 1992, Geometric-optical bidirectional reflectance modeling of the discrete crown vegetation canopy: Effect of crown shape and mutual shadowing. *IEEE Transactions on Geoscience and Remote Sensing*, **30**, pp. 276–292.

MEYER, P., ITTEN, K.I., KELLENBERGER, T., SANDMEIER, S. and SANDMEIER, R., 1993, Radiometric corrections of topographically induced effects on Landsat TM data in an alpine envrionment. *ISPRS Journal of Photogrammetry and Remote Sensing*, **48**, pp. 17–28.

MINNAERT, M., 1941, The reciprocity principle in lunar photometry. *Astrophysics Journal*, **93**, pp. 403–410.

PEDDLE, D.R., 1998, Field spectroradiometer data acquisition and processing for spectral mixture analysis in forestry and agriculture. In *Proceedings of the First International Conference on Geospatial Information in Agriculture and Forestry*, 1–3 June 1998, Lake Buena Vista, FL, USA.

PEDDLE, D.R., FRANKLIN, S.E., JOHNSON, R.L., LAVIGNE, M.A. and WULDER, M.A., 2003b, Structural change detection in a disturbed conifer forest using a geometric optical reflectance model in Multiple-Forward-Mode. *IEEE Transactions on Geoscience and Remote Sensing*, **41**, pp. 163–166.

PEDDLE, D.R., HALL, F.G. and LEDREW, E.F., 1999, Spectral mixture analysis and geometric optical reflectance modeling of boreal forest biophysical structure. *Remote Sensing of Environment*, **67**, pp. 288–297.

PEDDLE, D.R., JOHNSON, R.L., CIHLAR, J. and LATIFOVIC, R., 2004, Large area forest classification and biophysical parameter estimation using the 5-Scale canopy reflectance model in Multiple-Forward-Mode. *Remote Sensing of Environment*, **89**, pp. 252–263.

PEDDLE, D.R., JOHNSON, R.L., CIHLAR, J., LEBLANC, S.G. and CHEN, J.M., 2000, MFM-5-Scale: A Physically-Based Inversion Modeling Approach for Unsupervised Cluster Labeling and Independent Landcover Classification and Description. In *Proceedings, 22nd Canadian Symposium on Remote Sensing*, Victoria, BC, Canadian Aeronautics and Space Institute, Ottawa, pp. 477–486.

PEDDLE, D.R., JOHNSON, R.L., CIHLAR, J., LEBLANC, S.G., CHEN, J.M. and HALL, F.G., 2007, Physically-based inversion modeling for unsupervised cluster labeling, independent forest classification and LAI estimation using MFM-5-Scale. *Canadian Journal of Remote Sensing*, **33**, pp. 214–225.

PEDDLE, D.R., LUTHER, J.E., PILGER, N. and PIERCEY, D., 2003c, Forest biomass estimation using a physically-based 3D-structural modeling approach for Landsat TM cluster labeling. In *Proceedings, 25th Canadian Symposium on Remote Sensing*, 14–17 October 2003, Montreal, PQ, Canada (CD-ROM).

PEDDLE, D.R., TEILLET, P.M. and WULDER, M.A., 2003a, Radiometric image processing. Chapter 7. In *Remote Sensing of Forest Environments: Concepts and Case Studies*, M.A. Wulder and S.E. Franklin (Eds), pp. 181–208 (Norwell, MA: Kluwer Academic Press, 2003a).

PEDDLE, D.R., WHITE, H.P., SOFFER, R.J., MILLER, J.R. and LEDREW, E.F., 2001, Reflectance processing of remote sensing spectroradiometer data. *Computers and Geosciences*, **27**, pp. 203–213.

PILGER, N., PEDDLE, D.R. and HALL, R.J., 2003, Forest volume estimation using a canopy reflectance model in Multiple-Forward-Mode. In *Proceedings, 25th Canadian Symposium on Remote Sensing*, 14–17 October 2003, Montreal, PQ, Canada (CD-ROM).

SCHAAF, C.B., LI, X. and STRAHLER, A.H., 1992, Topographic effects on bidirectional and hemispherical reflectances calculated with a geometric-optical canopy model. IEEE *Transactions on Geoscience and Remote Sensing*, **32**, pp. 1186–1193.

SCHAFF, C.B. and STRAHLER, A.H., 1994, Validation of bidirectional and hemispherical reflectances from a geometric-optical model using ASAS imagery and pyranometer measurements of a spruce forest. *Remote Sensing of Environment*, **49**, pp. 138–144.

SMITH, J.A., LIN, T.L. and RANSON, K.J., 1980, The Lambertian assumption and Landsat data. *Photogrammetric Engineering and Remote Sensing*, **46**, pp. 1183–1189.

SMITH, G.M. and MILTON, E.J., 1999, The use of the empirical line method to calibrate remotely sensed data to reflectance. *International Journal of Remote Sensing*, **20**, pp. 2653–2662.

SOENEN, S.A., PEDDLE, D.R. and COBURN, C.A., 2005, SCS+C: A modified Sun-Canopy-Sensor topographic correction in forested terrain. *IEEE Transactions on Geoscience and Remote Sensing*, **43**, pp. 2148–2159.

SOENEN, S.A., PEDDLE, D.R., COBURN, C.A., HALL, R.J. and HALL, F.G., 2007, Canopy reflectance model inversion in Multiple-Forward-Mode: Analysis of multiple solution sets. *IEEE Transactions on Geoscience and Remote Sensing*, submitted.

TEILLET, P.M., GUINDON, B. and GOODENOUGH, D.G., 1982, On the slope-aspect correction of multispectral scanner data. *Canadian Journal of Remote Sensing*, **8**, pp. 84–106.

VINCINI, M. and FRAZZI, E., 2003, Multitemporal evaluation of topographic normalization methods on deciduous forest TM data. *Photogrammetric Engineering and Remote Sensing*, **41**, pp. 2586–2590.